

# A direct design approach for strengthening simple-span beams with external post-tensioning

Kiang Hwee Tan  
and DeCheng Kong

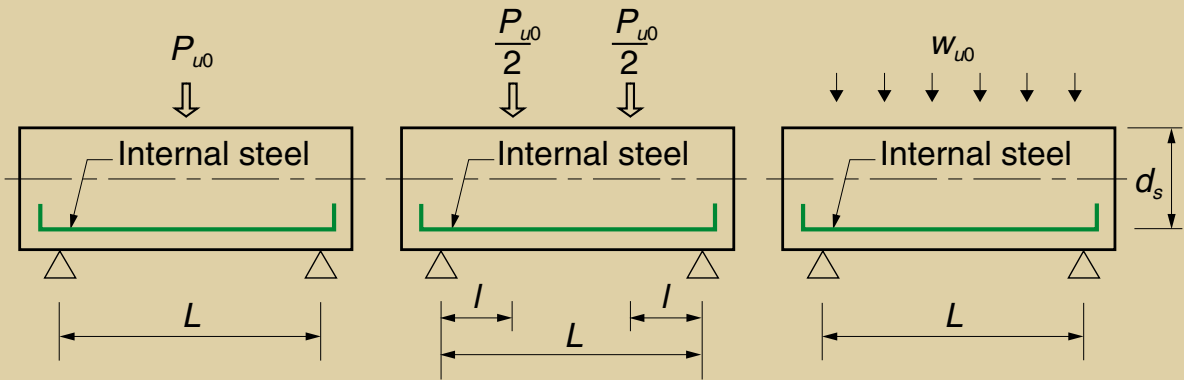
Structures may require strengthening due to aging or increases in design loads as a result of changes in usage. External post-tensioning is a technique used to strengthen concrete beams and girders because of ease of installation of the tendons and reduced or no interruptions to the regular function of the structure. An example of such a project is the rehabilitation of the Pier 39 parking structure in San Francisco, Calif.,<sup>1</sup> where the existing post-tensioned beams were strengthened by external post-tensioning. In this project, the anchors and deviators were fixed at night, and most of the stressing work was accomplished by jacking from the outside of the structure.

Because the tendons were placed on the exterior of the concrete beams, the analysis and design of the strengthened members were more complicated. External tendons are not bonded to the concrete, are free to move in between the deviators, and have a nearly constant stress along their lengths. The maximum tendon stress at the ultimate flexural-strength limit state of the beam is less than that of a beam with bonded tendons. Correspondingly, the load-carrying capacity of the beam is less.

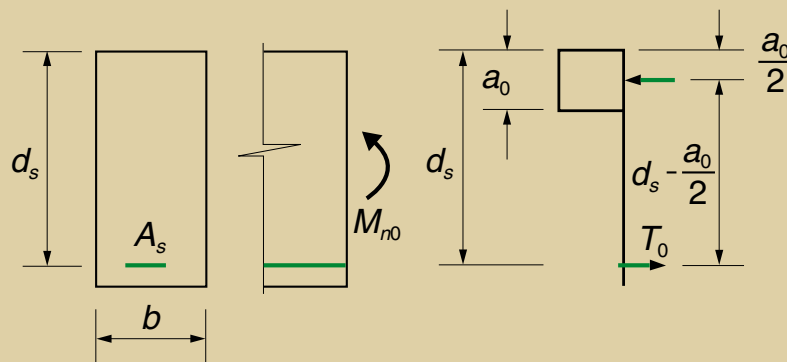
Although previous research<sup>2-4</sup> and existing codes<sup>5,6</sup> provided equations to evaluate the tendon stress at ultimate, allowing section analysis to be used in evaluating flexural strength, a more direct approach for determining the increase in load-carrying capacity due to the addition of external tendons is useful. Existing approaches consider the total load-carrying capacity of the strengthened beam.

## Editor's quick points

- This paper presents a direct approach to determine the tendon configuration for a desired increase in load-carrying capacity for simple-span beams.
- Two sets of equations—refined equations and simplified equations—are established for the determination of the increase in load-carrying capacity.
- A comparison of 124 simple-span beams from previous investigations showed that the increases in load-carrying capacity predicted by the refined equations are in good agreement with the test data, while the increases in load-carrying capacity predicted by the simplified equations are conservative.



Simple-span beam under symmetrical loadings



Moment capacity of critical section at midspan

**Figure 1.** These drawings illustrate the properties of unstrengthened beams. Note:  $a_0$  = depth of equivalent rectangular stress block for unstrengthened beam;  $A_s$  = area of tensile-steel reinforcement;  $b$  = beam width;  $d_s$  = effective depth of mild-steel reinforcement;  $l$  = distance from point load to nearest support;  $L$  = length of beam;  $M_{n0}$  = bending capacity of unstrengthened beam;  $P_{u0}$  = load-carrying capacity of unstrengthened beam;  $T_0$  = tensile force of reinforcement;  $w_{u0}$  = uniform load-carrying capacity of unstrengthened beam.

Alternatively, the new approach presented in this paper considers the increase in load-carrying capacity due to external post-tensioning and provides a more direct method for strengthening design.

This paper presents the analytical formulation to establish equations for the direct determination of the increase in load-carrying capacity of simple-span beams strengthened by external post-tensioned tendons. Two sets of equations—refined equations and simplified equations—are proposed. By using these equations, the tendon configuration in terms of its profile, area, and eccentricities can be determined for the strengthening of simple-span beams to carry a specified additional load. A design example is given in the appendix to illustrate the application of the method.

## Theoretical background

Consider a simple-span beam with a rectangular cross section (**Fig. 1**). Under symmetrical loads, such as a midspan concen-

trated load, third-point loads, or uniform load, the midspan section corresponds to the critical section in bending.

Assuming that the internal steel reinforcing bars yield at the ultimate limit state and ignoring compressive reinforcement, if any, the moment capacity of the critical midspan section  $M_{n0}$  is given by Eq. (1):

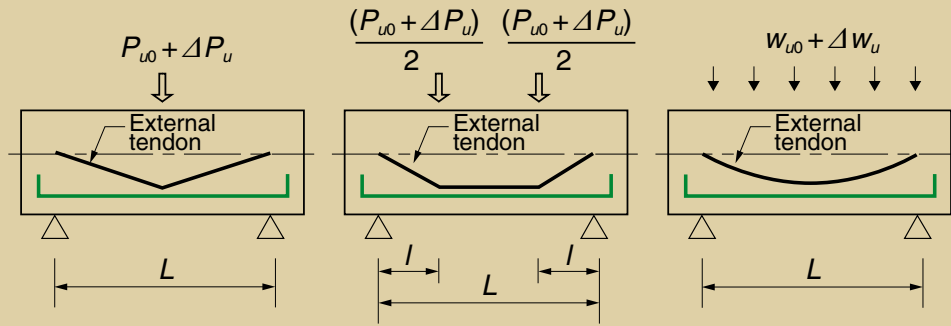
$$M_{n0} = T_0 \left( d_s - \frac{a_0}{2} \right) \quad (1)$$

where

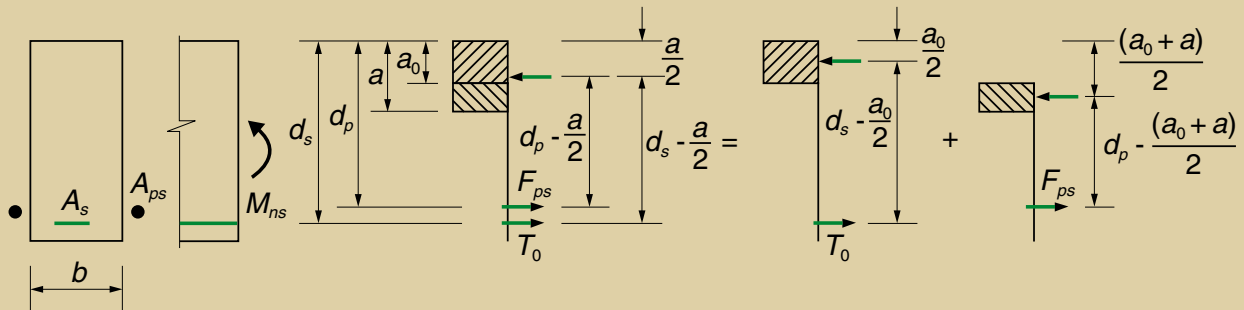
$T_0$  = force in tensile reinforcement

$d_s$  = effective depth of tensile-steel reinforcement

$a_0$  = depth of equivalent rectangular stress block for unstrengthened beams, which is given by Eq. (2)



Strengthened beams under symmetrical loadings



Moment capacity of critical section

**Figure 2.** These beams are strengthened with external tendons. Note:  $a$  = depth of equivalent rectangular stress block for strengthened beam;  $a_0$  = depth of equivalent rectangular stress block for unstrengthened beam;  $A_{ps}$  = area of prestressing steel;  $A_s$  = area of tensile-steel reinforcement;  $b$  = beam width;  $d_p$  = effective depth of prestressing tendon;  $d_s$  = effective depth of mild-steel reinforcement;  $F_{ps}$  = prestressing tendon force at ultimate limit state;  $l$  = distance from point load to nearest support;  $L$  = length of beam;  $M_{ns}$  = bending capacity of strengthened beam;  $P_{u0}$  = load-carrying capacity of unstrengthened beam;  $T_0$  = tensile force of reinforcement;  $w_{u0}$  = uniform load-carrying capacity of unstrengthened beam;  $\Delta P_u$  = increase in load-carrying capacity of strengthened beam;  $\Delta w_u$  = increase in uniform load.

$$a_0 = \frac{T_0}{0.85bf'_c} = \frac{A_s f_y}{0.85bf'_c} \quad (2)$$

$$M_{ns} = T_0 \left( d_s - \frac{a}{2} \right) + F_{ps} \left( d_p - \frac{a}{2} \right) \quad (3)$$

$$= T_0 \left( d_s - \frac{a_0}{2} \right) + F_{ps} \left( d_p - \frac{a_0 + a}{2} \right)$$

where

$b$  = beam width

$f'_c$  = concrete compressive strength

$A_s$  = area of mild-steel reinforcement

$f_y$  = yield strength of the internal tensile reinforcement

After the addition of external tendons, the flexural capacity of the critical section will increase from  $M_{n0}$  to  $M_{ns}$  (Fig. 2). Again, assume yielding of the internal reinforcement at ultimate limit state and no friction between the tendons and deviators. The moment capacity of the critical section shown in Fig. 2 can be expressed as Eq. (3).

where

$M_{ns}$  = moment capacity of strengthened beam

$F_{ps}$  = prestressing tendon force

$d_p$  = effective depth of external tendon

$a$  = depth of equivalent rectangular stress block for strengthened beam, which is given by Eq. (4)

$$a = \frac{T_0 + F_{ps}}{0.85bf'_c} = \frac{A_{ps} f_{ps} + A_s f_y}{0.85bf'_c} \quad (4)$$

where

$A_{ps}$  = area of prestressing steel

$f_{ps}$  = prestressing tendon stress

In view of Eq. (1) and (3), the increase in moment capacity  $\Delta M_n$  of the critical midspan section is calculated from Eq. (5).

$$\Delta M_n = M_{ns} - M_{n0} = F_{ps} \left( d_p - \frac{a_0 + a}{2} \right) \quad (5)$$

The effective tendon depth  $d_p$  at midspan is given by Eq. (6).

$$d_p = e_m + y_t \quad (6)$$

where

$e_m$  = eccentricity of prestressed tendon at midspan section

$y_t$  = distance between extreme concrete compression fiber and centroid of the section

The ratio of compression-stress-block depths  $K$  is determined from Eq. (7):

$$K = \frac{a}{a_0} \quad (7)$$

Equation (5) can be written as Eq. (8).

$$\Delta M_n = F_{ps} \left[ e_m + y_t - \frac{a_0}{2} (1 + K) \right] \quad (8)$$

An upper limit can be imposed on the value of  $K$  by requiring the strengthened beam to remain underreinforced in flexure—that is, failure to be tension controlled. For this to occur, the American Concrete Institute (ACI) *Building Code Requirements for Structural Concrete (ACI 318-08) and Commentary (ACI 318R-08)*<sup>5</sup> specifies that the net tensile strain in the extreme tension steel at nominal strength shall be equal to or greater than 0.005, which requires

$$\frac{a}{\beta_1 d_s} \leq 0.375$$

where

$\beta_1$  = factor that defines depth of equivalent rectangular stress block as function of the neutral-axis depth

$\frac{a}{\beta_1}$  = depth of neutral axis of section

Substituting  $a$  as  $0.375\beta_1 d_s$  into Eq. (7) gives Eq. (9).

$$K = \frac{0.375\beta_1 d_s}{a_0} \quad (9)$$

Alternatively, substituting Eq. (2) and (4) into (7) gives Eq. (10) to determine the value of  $K$ .

$$\begin{aligned} K &= \frac{A_{ps} f_{ps} + A_s f_y}{A_s f_y} = 1 + \frac{A_{ps} f_{ps}}{A_s f_y} \\ &= 1 + \frac{\rho_p f_{ps} d_p}{\rho_s f_y d_s} \end{aligned} \quad (10)$$

where

$\rho_p$  = prestressing steel ratio

$$= \frac{A_{ps}}{b d_p}$$

$\rho_s$  = tensile-steel reinforcement ratio

$$= \frac{A_s}{b d_s}$$

Because  $f_{ps}$  is less than or equal to  $f_{py}$ , where  $f_{py}$  is the yield strength of prestressing steel (which corresponds to the stress at a total strain of 1% for wires and strands and 0.7% for bars), another upper-limit value of  $K$  is given by substituting  $f_{py}$  for  $f_{ps}$  into Eq. (10), which gives Eq. (11).

$$K = 1 + \chi \frac{d_p}{d_s} \quad (11)$$

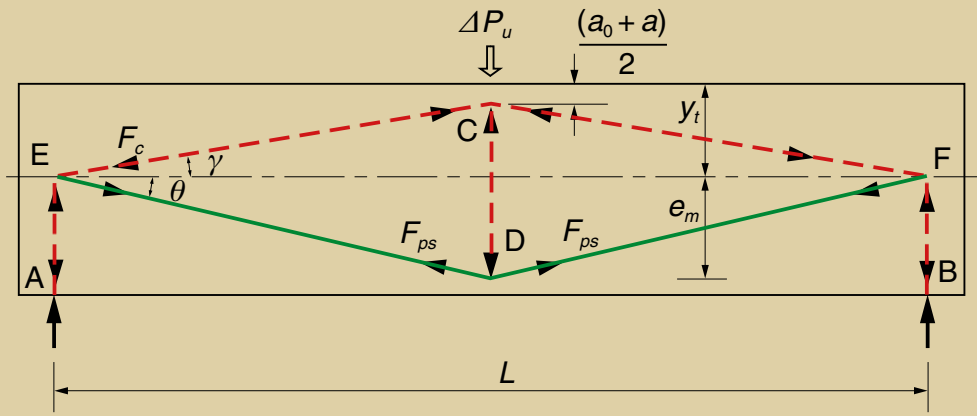
where

$\chi$  = relative prestressing index, which is given by Eq. (12)

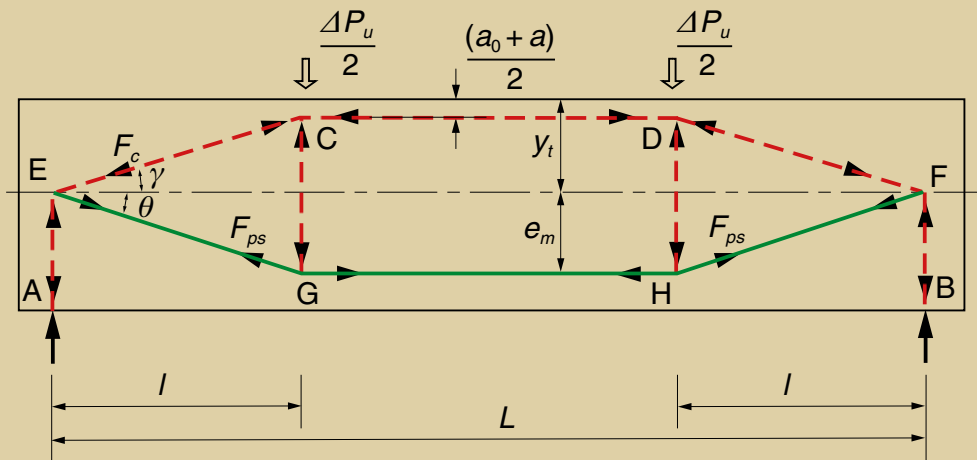
$$\chi = \frac{\rho_p f_{py}}{\rho_s f_y} \quad (12)$$

## Strength enhancement due to external tendons

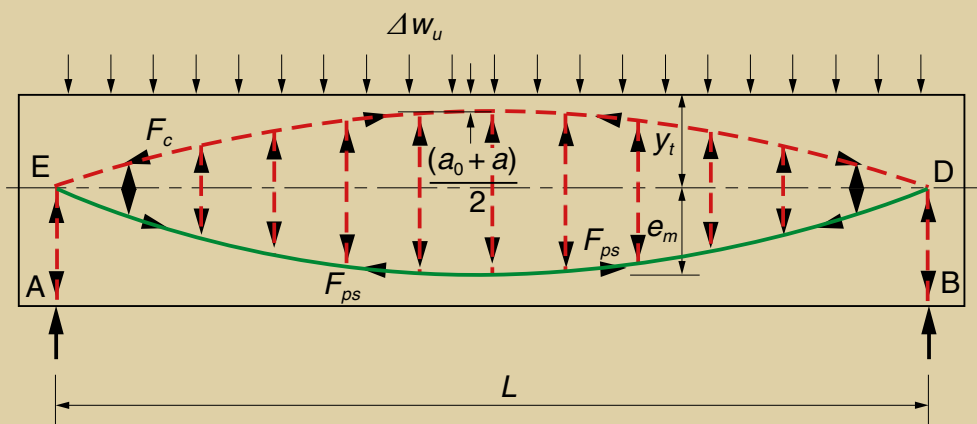
In the load-balancing method of design,<sup>7</sup> the prestressing tendon profile is chosen such that the moment diagram due to the prestressing force matches that due to the applied loads. The same concept of matching the tendon profile to the load pattern can be used for beam strengthening with external tendons (Fig. 2). For simple-span beams carrying a point load at midspan, tendons draped at midspan are used. For simple-span beams carrying two point loads, tendons double draped at the loading points are required. For simple-span beams carrying a uniform load, parabolic tendons are desirable.



Singly draped tendon



Doubly draped tendon



Parabolic tendon

**Figure 3.** These drawings illustrate the different strut-and-tie models. Note:  $a$  = depth of equivalent rectangular stress block for strengthened beam;  $a_0$  = depth of equivalent rectangular stress block for unstrengthened beam;  $e_m$  = eccentricity of prestressing tendon at midspan;  $F_c$  = concrete strut force;  $F_{ps}$  = prestressing tendon force at ultimate limit state;  $l$  = distance from point load to nearest support;  $L$  = length of beam;  $y_t$  = distance between extreme compressive fiber and centroidal axis of beam before cracking;  $\gamma$  = angle between strut and centroidal axis of the beam;  $\Delta P_u$  = increase in load-carrying capacity of strengthened beam;  $\Delta w_u$  = increase in uniform load;  $\theta$  = angle between tendon and centroidal axis of the beam.

Once the increase in moment capacity of the critical midspan section has been determined from Eq. (8) and (9) or (11), the increase in load-carrying capacity  $\Delta P_u$  of the beam can be calculated by considering moment equilibrium at critical section.

For beams subjected to a midspan point load,

$$\Delta M_n = \frac{\Delta P_u L}{4}$$

where

$L$  = length of beam

This gives Eq. (13).

$$\Delta P_u = 4F_{ps} \frac{e_m}{L} + 4F_{ps} \frac{y_t - \frac{a_0}{2}(1+K)}{L} \quad (13)$$

For beams subjected to two symmetrical point loads,

$$\Delta M_n = \frac{\Delta P_u L}{2}$$

where

$l$  = distance from point load to nearest support

This gives Eq. (14).

$$\Delta P_u = 2F_{ps} \frac{e_m}{l} + 2F_{ps} \frac{y_t - \frac{a_0}{2}(1+K)}{l} \quad (14)$$

For beams under uniform load,

$$\Delta M_n = \frac{\Delta w_u L^2}{8}$$

where

$\Delta w_u$  = increase in uniform load

This gives Eq. (15).

$$\Delta P_n = \Delta w_u L = \frac{8F_{ps} e_m}{L} + \frac{8F_{ps} \left[ y_t - \frac{a_0}{2}(1+K) \right]}{L} \quad (15)$$

Equations (13)–(15) can also be derived by considering strut-and-tie models (**Fig. 3**). The node C is located below the loading point at middepth of the compression zone attributed to the external tendons (Fig. 2). By considering the vertical-force equilibrium at node C (Fig. 3), the increase in load-carrying capacity is determined by Eq. (16).

$$\Delta P_u = 2F_{ps} \sin \theta + 2F_{ps} \cos \theta \tan \gamma \quad (16)$$

where

$\theta$  = angle between tendon and centroidal axis of the beam

$\gamma$  = angle between the centroidal axis of the beam and strut

$$\tan \theta = \frac{e_m}{L/2} \quad (17)$$

$$\tan \gamma = \frac{y_t - \frac{a_0 + a}{2}}{L/2} = \frac{y_t - \frac{a_0}{2}(1+K)}{L/2} \quad (18)$$

Assuming small values of  $\theta$ , then the terms  $\sin \theta$  and  $\cos \theta$  in Eq. (16) can be replaced by  $\tan \theta$  and 1, respectively. Substituting the values of  $\tan \theta$  and  $\tan \gamma$  from Eq. (17) and (18) into Eq. (16) gives the same result as Eq. (13). Using the same procedure, Eq. (14) can be obtained for beams subjected to two symmetrical point loads (Fig. 3), and Eq. (15) can be derived for beams under uniform load.

Equations (13)–(15) each consist of two terms. The first term corresponds to the load balanced directly by the tendons. The second term arises from the increase in concrete compression zone. These are called refined equations in this paper.

Omitting the second term in Eq. (13)–(15) leads to Eq. (19)–(21).

For beams subjected to a midspan point load

$$\Delta P_u = 4F_{ps} \frac{e_m}{L} \quad (19)$$

For beams subjected to two symmetrical point loads

$$\Delta P_u = 2F_{ps} \frac{e_m}{l} \quad (20)$$

For beams under uniform load

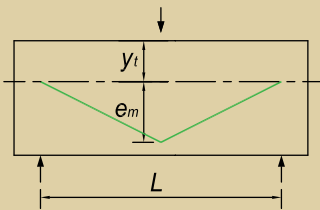
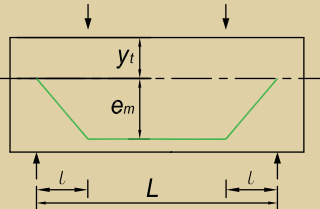
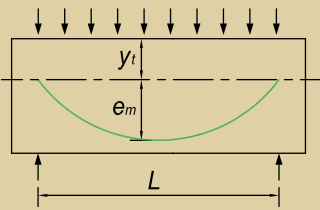
$$\Delta P_u = \frac{8F_{ps} e_m}{L} \quad (21)$$

These equations give conservative estimates of the increase in load-carrying capacity. These are called simplified equations, which are dependent on the tendon profiles only and are independent of the properties of the original beam. **Table 1** summarizes the set of refined and simplified equations.

## Tendon stress

To use the refined or simplified equations either to deter-

**Table 1.** Refined and simplified equations for increase in load-carrying capacity

	Refined equations	Simplified equations
	$\Delta P_u = 4F_{ps} \frac{e_m}{L} + 4F_{ps} \frac{y_t - \frac{a_0}{2}(1+K)}{L} \text{ Eq. (13)}$	$\Delta P_u = 4F_{ps} \frac{e_m}{L} \text{ Eq. (19)}$
	$\Delta P_u = 2F_{ps} \frac{e_m}{l} + 2F_{ps} \frac{y_t - \frac{a_0}{2}(1+K)}{l} \text{ Eq. (14)}$	$\Delta P_u = 2F_{ps} \frac{e_m}{l} \text{ Eq. (20)}$
	$\Delta P_u = \Delta w_u L = \frac{8F_{ps}e_m}{L} + \frac{8F_{ps} \left[ y_t - \frac{a_0}{2}(1+K) \right]}{L} \text{ Eq. (15)}$	$\Delta P_u = \frac{8F_{ps}e_m}{L} \text{ Eq. (21)}$

Note:  $a_0$  = depth of equivalent rectangular stress block for unstrengthened beam;  $e_m$  = eccentricity of prestressing tendon at midspan;  $F_{ps}$  = prestressing tendon force at ultimate limit state;  $K$  = ratio of compression-stress-block depths;  $l$  = distance from point load to nearest support;  $L$  = beam span;  $y_t$  = distance between extreme compressive fiber and centroidal axis of the beam before cracking;  $\Delta P_u$  = increase in load-carrying capacity due to the addition of external tendons;  $\Delta w_u$  = increase in uniform load.

mine  $\Delta P_u$  due to the provision of the external tendons or the tendon area  $A_{ps}$  required to carry the additional load  $\Delta P_u$ , the tendon stress  $f_{ps}$  at ultimate flexural limit state must be known. Three equations that have been proposed for  $f_{ps}$  are considered.

### ACI 318-08 equation

The tendon stress is given by Eq. (22).<sup>5</sup>

$$f_{ps} = f_{pe} + 68.95 + \frac{f'_c}{B\rho_p} \quad (22)$$

where

$$f_{ps} \leq f_{pe} + C$$

$$f_{ps} \leq f_{py}$$

$f_{pe}$  = effective stress of prestressing tendon

$B$  = constant

$C$  = constant

For  $L/d_p \leq 35$ , the constant  $B$  is 100 and the constant  $C$  is 414. For  $L/d_p > 35$ ,  $B$  is 300 and  $C$  is 207.

### MacGregor's equation

The tendon stress is calculated using Eq. (23).<sup>8,9</sup>

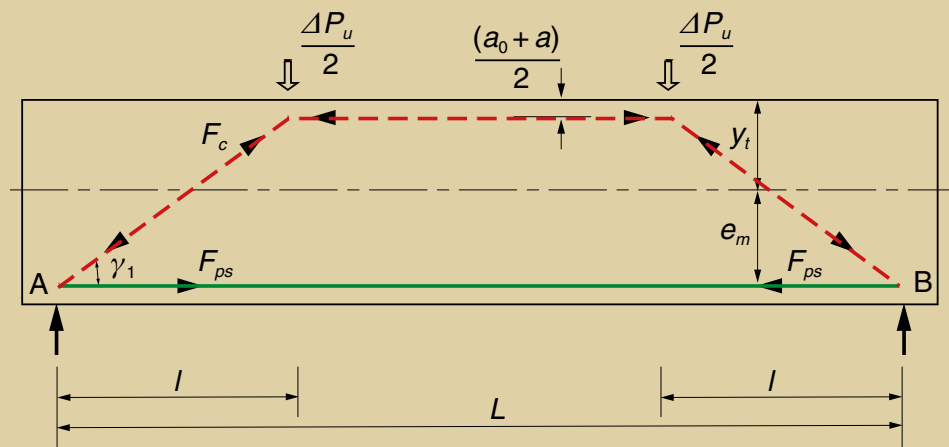
$$f_{ps} = f_{pe} + 0.0315E_{ps} \frac{d_p - c}{L} \leq f_{py} \quad (23)$$

where

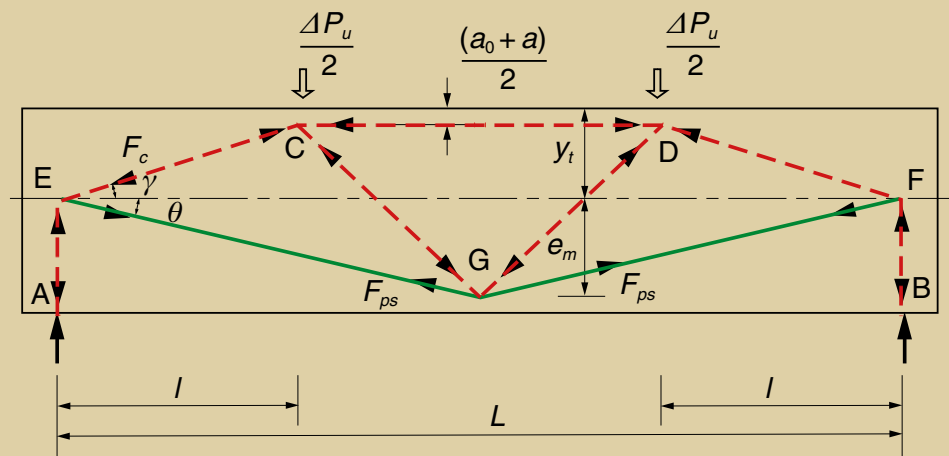
$c$  = neutral-axis depth of strengthened beam at critical midspan section

$$= \frac{a}{\beta_1}$$

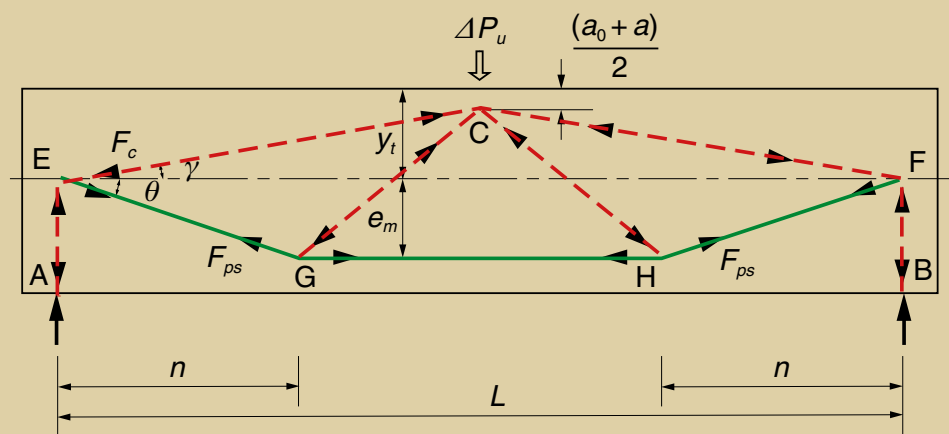
$E_{ps}$  = elastic modulus of prestressing tendon



With straight tendon under two-point load



With singly draped tendon under two-point load



With doubly draped tendon under single-point load

**Figure 4.** These are simple-span beams that carry nonmatching loads. Note:  $a$  = depth of equivalent rectangular stress block for strengthened beam;  $a_0$  = depth of equivalent rectangular stress block for unstrengthened beam;  $e_m$  = eccentricity of prestressing tendon at midspan;  $F_c$  = concrete strut force;  $F_{ps}$  = prestressing tendon force at ultimate limit state;  $l$  = distance from point load to nearest support;  $L$  = length of beam;  $n$  = distance from draped point to nearest support;  $y_t$  = distance between most compressive fiber and centroidal axis of beam before cracking;  $\gamma$  = angle between strut and centroidal axis of the beam;  $\gamma_1$  = angle between the straight tendon and the inclined strut for strengthened beam;  $\Delta P_u$  = increase in load-carrying capacity due to addition of external tendons;  $\theta$  = angle between tendon and centroidal axis of the beam.



**Table 2.** Characteristics of simple-span beams studied by Tan et al.

Beam marking	$\rho_s$ , %	$f'_c$ , MPa	$A_{ps}$ , mm <sup>2</sup>	$f_{pe}$ , MPa	$f_{pu}$ , MPa	$e_s$ , mm	$e_m$ , mm	$L/d_p$	Number of deviators	Profile*	Load type†
T-1	0.51	34.2	110	1197	1900	78	78	15.0	1	S	T
T-1A	0.51	30.4	110	327	1900	128	128	12.0	1	S	T
T-1D	0.51	32.1	110	288	1900	0	128	12.0	1	SD	T
T-1B	0.51	33.2	201	750	1900	78	78	15.0	1	S	T
ST-1	0.51	34.5	201	764	1900	78	78	7.5	1	S	T
ST-2	0.51	29.9	201	771	1900	78	78	9.0	1	S	T
ST-4	0.51	28.3	201	757	1900	78	78	22.5	1	S	T
ST-5	0.51	25.1	201	760	1900	78	78	30.0	1	S	T
T-0	0.51	34.6	110	1297	1900	78	78	15.0	0	S	T
T-2	0.51	28.7	110	1182	1900	78	78	15.0	2	S	T
T-0A	0.51	31.3	110	745	1900	78	78	22.5	0	S	T
T-0B	0.51	29.3	110	742	1900	78	78	30.0	0	S	T
ST-5A	0.51	31.7	201	762	1900	78	78	30.0	2	S	T
ST-5B	0.51	26.4	201	742	1900	78	78	30.0	3	S	T
SR2	1.24	27.0	201	1023	1900	0	200	9.1	1	SD	T
SR4	1.24	24.2	201	1283	1900	0	200	9.1	1	SD	T
SR5	0.33	23.7	201	1060	1900	0	80	14.3	1	SD	T
SR6	1.24	28.0	201	1079	1900	0	80	14.3	1	SD	T
SR1A	0.33	24.0	110	1023	1900	0	140	11.1	1	SD	T
SR1B	0.33	21.0	201	1023	1900	0	140	11.1	1	SD	T
SR3A	0.33	23.7	110	1023	1900	0	80	14.3	1	SD	T
SR3B	0.33	24.1	201	1302	1900	0	140	11.1	1	SD	T
SR7	0.33	24.0	201	1023	1900	0	80	14.3	1	SD	S

Sources: Data from Tan and Ng 1997; Tan, Naaman, Mansur, and Ng 1997.

\* S = straight; SD = singly draped.

† S = single-point load; T = two-point loads.

Note:  $A_{ps}$  = area of prestressing tendon;  $d_p$  = effective depth of prestressing tendon;  $e_m$  = eccentricity of tendon at midspan;  $e_s$  = eccentricity of prestressing tendon at support;  $f'_c$  = concrete compressive strength;  $f_{pe}$  = effective stress of the prestressing tendon;  $f_{pu}$  = ultimate stress of prestressing tendon;  $L$  = length of beam;  $\rho_s$  = tensile-steel reinforcement ratio. 1 mm = 0.0394 in.; 1 MPa = 0.145 ksi.

Incorporating Eq. (7) into Eq. (23) and substituting for  $c$  results in Eq. (24).

$$f_{ps} = f_{pe} + 0.0315E_{ps} \frac{d_p - Ka_0 / \beta_1}{L} \leq f_{py} \quad (24)$$

### Naaman's equation

The tendon stress is given by Eq. (25).<sup>4</sup>

$$f_{ps} = f_{pe} + \Omega_u E_{ps} \epsilon_{ce} + \Omega_u E_{ps} \frac{d_p - c}{c} \epsilon_{cu} \quad (25)$$

**Table 3.** Characteristics of simple-span beams studied by Tan

Beam marking	$\rho_{st}$ %	$f'_c$ MPa	$A_{ps}$ mm <sup>2</sup>	$f_{pe}$ MPa	$f_{pu}$ MPa	$e_s$ mm	$e_m$ mm	$L/d_p$	Number of deviators	Profile*	Load type†
TD1	0.52	32.8	200	980	1900	0	80	14.2	2	DD	T
TD2	0.52	33.6	110	969	1900	0	135	11.1	2	DD	T
TD3	0.52	33.6	200	975	1900	0	135	11.1	2	DD	T
TD4	0.52	43.2	200	1000	1900	50	135	11.1	2	DD	T
TP1	0.52	32.8	200	980	1900	0	135	11.1	4	P	U

Source: Data from Tan 2006.

\* DD = doubly draped; P = parabolic.

† T = two-point loads; U = uniform load.

Note:  $A_{ps}$  = area of prestressing tendon;  $d_p$  = effective depth of prestressing tendon;  $e_m$  = eccentricity of tendon at midspan;  $e_s$  = eccentricity of prestressing tendon at support;  $f'_c$  = concrete compressive strength;  $f_{pe}$  = effective stress of the prestressing tendon;  $f_{pu}$  = ultimate stress of prestressing tendon;  $L$  = length of beam;  $\rho_s$  = tensile-steel reinforcement ratio. 1 mm = 0.0394 in.; 1 MPa = 0.145 ksi.

where

$\epsilon_{ce}$  = precompression strain in concrete at tendon level

$\epsilon_{cu}$  = ultimate concrete compression strain

$\Omega_u$  = bond reduction factor, which for simple-span beams is given by Eq. (26) and (27)

$$\Omega_u = \frac{2.6}{L/d_p} \quad (\text{for a single point load}) \quad (26)$$

$$\Omega_u = \frac{5.4}{L/d_p} \quad (\text{for two point loads or a uniform load}) \quad (27)$$

Again incorporating Eq. (7) and substituting for  $c$ , Eq. (25) can be written as Eq. (28).

$$f_{ps} = f_{pe} + \Omega_u E_{ps} \epsilon_{ce} + \Omega_u E_{ps} \left( \frac{d_p \beta_1}{K a_0} - 1 \right) \epsilon_{cu} \quad (28)$$

## Application to non-load-matching tendons

In Fig. 2, the external tendons are arranged such that the bending moment at sections along the beam length are equal to and opposite of the bending moments due to the increased external load. Such tendons are called load-matching tendons in this study. For beams provided with non-load-matching tendons, the equations to calculate the increase in load-carrying capacity are obtained using the strut-and-tie models in Fig. 4.

Figure 4 shows a beam with straight tendons carrying two point loads. The increase in load-carrying capacity can be determined by considering force equilibrium at nodes C or D. Equation (29) calculates this value.

$$\frac{\Delta P_u}{2} = F_{ps} \tan \gamma_1 \quad (29)$$

where

$\gamma_1$  = angle between the straight tendon and the inclined strut AC (Fig. 4), which is given by Eq. (30)

$$\tan \gamma_1 = \frac{e_m + y_t - \frac{a_0 + a}{2}}{l} = \frac{e_m + y_t - \frac{a_0}{2}(1+K)}{l} \quad (30)$$

Substituting  $\tan \gamma_1$  from Eq. (30) into (29) and rearranging gives Eq. (31).

$$\Delta P_u = 2F_{ps} \frac{e_m}{l} + 2F_{ps} \frac{y_t - \frac{a_0}{2}(1+K)}{l} \quad (31)$$

This is the same as Eq. (14). Thus, there is no difference between the increase in load-carrying capacity for a straight or double-draped tendon.

For a beam with a single-draped tendon under two point loads (Fig. 4), vertical force equilibrium at nodes C and G gives Eq. (32).

$$\Delta P_u = 4F_{ps} \frac{e_m}{L} + 2F_{ps} \frac{y_t - \frac{a_0}{2}(1+K)}{l} \quad (32)$$

**Table 4.** Characteristics of simple-span beams studied by Harajli

Beam marking	$\rho_s$ %	$f'_c$ , MPa	$A_{ps}$ , mm <sup>2</sup>	$f_{pe}$ , MPa	$f_{pu}$ , MPa	$e_s$ , mm	$e_m$ , mm	$L/d_p$	Number of deviators	Profile*	Load type†
B4D	0.60	30.3	38.7	879	1606	0	161	10.9	1	SD	T
B4S	0.60	27.6	38.7	972	1606	80	80	15.4	0	S	T
B5D	1.33	32.4	77.4	841	1427	0	162	10.8	1	SD	T
B5S	1.33	37.8	77.4	789	1427	80	80	15.4	0	S	T
B6D	1.80	33.8	77.4	765	1427	0	162	10.8	1	SD	T

Source: Data from Harajli 1993.

\* S = straight; SD = singly draped.

† T = two-point loads.

Note:  $A_{ps}$  = area of prestressing tendon;  $d_p$  = effective depth of prestressing tendon;  $e_m$  = eccentricity of tendon at midspan;  $e_s$  = eccentricity of prestressing tendon at support;  $f'_c$  = concrete compressive strength;  $f_{pe}$  = effective stress of the prestressing tendon;  $f_{pu}$  = ultimate stress of prestressing tendon;  $L$  = length of beam;  $\rho_s$  = tensile-steel reinforcement ratio. 1 mm = 0.0394 in.; 1 MPa = 0.145 ksi.

**Table 5.** Characteristics of simple-span beams studied by Khairallah and Harajli

Beam marking	$\rho_s$ %	$f'_c$ , MPa	$A_{ps}$ , mm <sup>2</sup>	$f_{pe}$ , MPa	$f_{pu}$ , MPa	$e_s$ , mm	$e_m$ , mm	$L/d_p$	Number of deviators	Profile*	Load type†
T1S	0.26	39.6	77	788	1427	84	84.0	14.6	0	S	T
T1D	0.26	40.8	77	792	1427	84	228.6	8.6	1	SD	T
T2S	0.40	40.1	39	935	1607	84	84.0	14.6	0	S	T
T2D	0.40	43.5	39	931	1607	84	228.6	8.6	1	SD	T
T3S	0.54	37.9	77	747	1427	84	84.0	14.6	0	S	T
T3D	0.54	39.0	77	895	1427	84	228.6	8.6	1	SD	T
T4S	0.71	41.8	75	994	1986	84	84.0	14.6	0	S	T
T4D	0.71	38.7	75	1001	1986	84	228.6	8.6	1	SD	T

Source: Data from Khairallah and Harajli 1997.

\* S = straight; SD = singly draped.

† T = two-point loads.

Note:  $A_{ps}$  = area of prestressing tendon;  $d_p$  = effective depth of prestressing tendon;  $e_m$  = eccentricity of tendon at midspan;  $e_s$  = eccentricity of prestressing tendon at support;  $f'_c$  = concrete compressive strength;  $f_{pe}$  = effective stress of the prestressing tendon;  $f_{pu}$  = ultimate stress of prestressing tendon;  $L$  = length of beam;  $\rho_s$  = tensile-steel reinforcement ratio. 1 mm = 0.0394 in.; 1 MPa = 0.145 ksi.

For a beam with double-draped tendons carrying a single point load,  $\Delta P_u$  is determined by Eq. (33).

$$\Delta P_u = 2F_{ps} \frac{e_m}{n} + 4F_{ps} \frac{y_t - \frac{a_0}{2}(1+K)}{L} \quad (33)$$

where

$n$  = distance from draped point to the nearest support

## Verification of proposed equations

Test results from existing literature were used to verify the proposed equations. These include test results of externally prestressed beams and internally post-tensioned beams with unbonded tendons, which exhibit responses similar to externally prestressed beams. A total of 124 simple-span beams from previous researchers<sup>10–23</sup> were considered. The beams comprised rectangular and T-beams with span-to-depth ratios  $L/d_p$  varying from 7.5 to 55.2, and reinforcement ratios  $\rho_s$  from 0.11% to 2.44%. The tendon profiles include straight, single-draped, double-draped, and parabolic profiles. **Tables 2–11** show the details.

The load-carrying capacities of the unstrengthened beams  $P_{u0}$  were first calculated using conventional flexural theory based on strain compatibility. The observed increase in

load-carrying capacity  $\Delta P_{us}$  was obtained by deducting  $P_{u0}$  from the observed load-carrying capacity of the strengthened beams  $P_{us}$ .

The predicted increases in load-carrying capacity of the strengthened beam  $\Delta P_{u, pred}$  based on refined equations and simplified equations are denoted as  $\Delta P_{u1X}$  and  $\Delta P_{u2X}$ , respectively. The subscript  $X$  is equal to 1, 2, or 3, indicating the equations with which the tendon stress is evaluated—that is, ACI 318-05 Eq. (22), MacGregor Eq. (24), or Naaman Eq. (28), respectively.

**Table 12** summarizes the mean and standard deviation of  $\Delta P_{us}/\Delta P_{u, pred}$ . The predicted increase in load-carrying capacities is plotted against the observed values in **Fig. 5** and **6** for values of  $K$  given by Eq. (9) and (11), respectively.

**Table 6.** Characteristics of simple-span beams studied by Harajli and Kanj

Beam marking	$\rho_s$ , %	$f'_c$ , MPa	$A_{ps}$ , mm <sup>2</sup>	$f_{pe}$ , MPa	$f_{pu}$ , MPa	$e_s$ , mm	$e_m$ , mm	$L/d_p$	Profile*	Load type†
PP2R3-3	0.60	43.2	38.7	952	1482	44.5	44.5	19.2	S	T
PP2R3-0	0.60	43.8	38.7	938	1482	44.5	44.5	19.2	S	S
PP3R3-3	0.88	43.2	77.4	883	1427	44.5	44.5	19.2	S	T
PP3R3-0	0.88	39.0	77.4	896	1427	44.5	44.5	19.2	S	S
P1R3-3	0.22	44.4	19.4	1014	1606	44.5	44.5	19.2	S	T
P1R3-0	0.22	41.7	19.4	993	1606	44.5	44.5	19.2	S	S
P2R3-3	0.22	46.9	77.4	858	1482	44.5	44.5	19.2	S	T
P2R3-0	0.22	38.6	77.4	872	1427	44.5	44.5	19.2	S	S
P3R3-3	0.22	46.5	116.1	879	1427	44.5	44.5	19.2	S	T
P3R3-0	0.22	41.2	116.1	845	1427	44.5	44.5	19.2	S	S
PP1R2-3	0.48	42.2	38.7	862	1482	69.9	69.9	12.1	S	T
PP1R2-0	0.48	41.9	38.7	827	1482	69.9	69.9	12.1	S	S
PP2R2-3	0.70	42.1	77.4	879	1482	69.9	69.9	12.1	S	T
PP2R2-0	0.70	38.1	77.4	872	1482	69.9	69.9	12.1	S	S
PP3R2-3	0.96	42.5	116.1	886	1482	69.9	69.9	12.1	S	T
PP3R2-0	0.96	44.4	116.1	917	1482	69.9	69.9	12.1	S	S

Source: Data from Harajli and Kanj 1991; Harajli and Kanj 1992.

\* S = straight.

† S = single-point load; T = two-point loads.

Note:  $A_{ps}$  = area of prestressing tendon;  $d_p$  = effective depth of prestressing tendon;  $e_m$  = eccentricity of tendon at midspan;  $e_s$  = eccentricity of prestressing tendon at support;  $f'_c$  = concrete compressive strength;  $f_{pe}$  = effective stress of the prestressing tendon;  $f_{pu}$  = ultimate stress of prestressing tendon;  $L$  = length of beam;  $\rho_s$  = tensile-steel reinforcement ratio. 1 mm = 0.0394 in.; 1 MPa = 0.145 ksi.

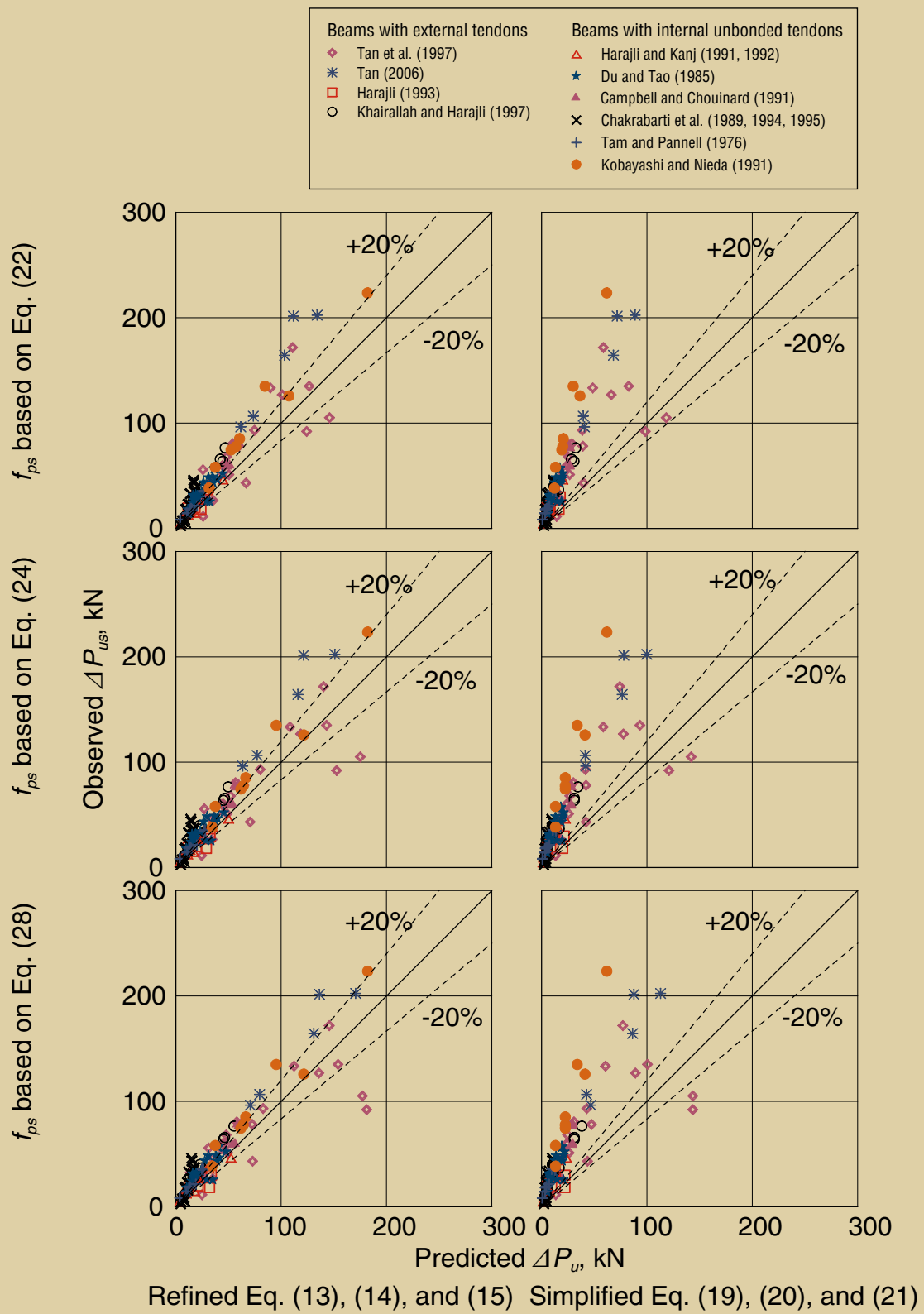
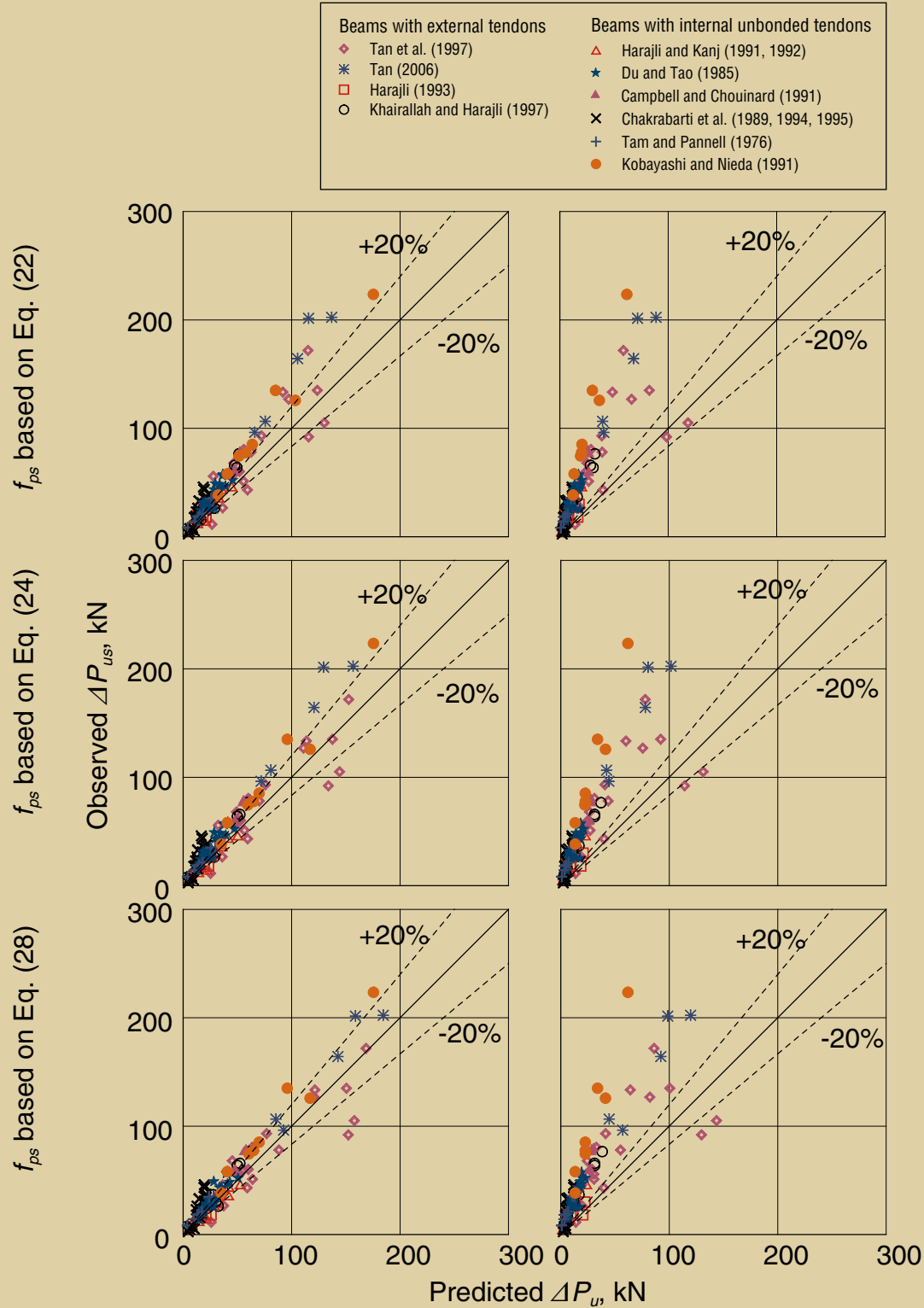


**Figure 5.** These graphs compare the predicted load increase using  $K = 0.375\beta_1 d_s/a_0$  with the test results. Note: The solid lines represent perfect correlation, and the dashed lines indicate a  $\pm 20\%$  deviation.  $a_0$  = depth of equivalent rectangular stress block for unstrengthened beam;  $d_s$  = effective depth of tensile-steel reinforcement;  $f_{ps}$  = prestressing tendon stress at ultimate limit state;  $K$  = ratio of compression-stress-block depths;  $\beta_1$  = factor to determine depth of equivalent rectangular stress block;  $\Delta P_u$  = increase in load-carrying capacity due to addition of external tendons;  $\Delta P_{us}$  = observed increase in load-carrying capacity. 1 kN = 0.225 kip.



Refined Eq. (13), (14), and (15) Simplified Eq. (19), (20), and (21)

**Figure 6.** These graphs compare the predicted load increase using  $K = 1 + \chi(d_p/d_s)$  with the test results. Note: The solid lines represent perfect correlation, and the dashed lines indicate a  $\pm 20\%$  deviation.  $d_p$  = effective depth of prestressing tendon;  $d_s$  = effective depth of tensile-steel reinforcement;  $f_{ps}$  = prestressing tendon stress at ultimate limit state;  $K$  = ratio of compression-stress-block depths;  $\Delta P_u$  = increase in load-carrying capacity due to addition of external tendons;  $\Delta P_{us}$  = observed increase in load-carrying capacity;  $\chi$  = relative prestressing index. 1 kN = 0.225 kip.

**Table 7.** Characteristics of simple-span beams studied by Chakrabarti et al.

Beam marking	$\rho_{st}$ %	$f'_c$ , MPa	$A_{ps}$ , mm <sup>2</sup>	$f_{pe}$ , MPa	$f_{pu}$ , MPa	$e_s$ , mm	$e_m$ , mm	$L/d_p$	Profile*	Load type†
A-2	0.25	34.5	46.4	1048	1860	0	50.8	21.2	DD	T
A-3	0.50	35.2	46.4	1069	1860	0	50.8	21.2	DD	T
B-2	0.50	36.0	69.7	993	1860	0	50.8	21.2	DD	T
B-3	1.16	36.6	46.4	1110	1860	0	50.8	21.2	DD	T
C-2	0.75	35.9	116.1	938	1860	0	38.1	23.0	DD	T
C-3	1.82	33.8	69.7	1110	1860	0	50.8	21.2	DD	T
PPT9A	0.11	60.7	46.4	1245	1860	0	105.9	18.4	DD	T
PPT9B	0.19	60.1	46.4	1245	1860	0	105.9	18.4	DD	T
PPT9C	0.49	51.4	46.4	1099	1860	0	105.9	18.4	DD	T
PPT9D	0.81	51.4	46.4	1096	1860	0	105.9	18.4	DD	T
PPT5A	0.19	37.8	46.4	1193	1860	0	105.9	18.4	DD	T
PPT5B	0.49	30.5	46.4	1173	1860	0	105.9	18.4	DD	T
PPR9A	1.16	54.4	46.4	1155	1860	0	50.8	21.2	DD	T
PPR9B	1.16	51.7	46.4	1173	1860	0	50.8	21.2	DD	T
K11	1.40	35.2	46.4	1289	1860	0	22.2	55.2	DD	T
K12	1.64	34.8	46.4	1303	1860	0	31.8	42.5	DD	T
K13	1.52	34.1	46.4	1324	1860	0	41.3	34.5	DD	T
K21	0.37	35.5	46.4	1289	1860	0	22.2	55.2	DD	T
K22	0.28	35.2	46.4	1282	1860	0	31.8	42.5	DD	T
K23	0.46	34.5	46.4	1303	1860	0	41.3	34.5	DD	T
E11	0.50	34.5	46.4	768	1860	0	50.8	21.2	DD	T
E12	0.50	34.4	46.4	892	1860	0	50.8	21.2	DD	T
E13	0.50	34.7	46.4	1132	1860	0	50.8	21.2	DD	T
E14	0.50	34.6	46.4	1322	1860	0	50.8	21.2	DD	T

Source: Data from Chakrabarti and Whang 1989; Chakrabarti, Whang, Brown, Arsad, and Amezeua 1994; Chakrabarti 1995.

\* DD = doubly draped.

† T = two-point loads.

Note:  $A_{ps}$  = area of prestressing tendon;  $d_p$  = effective depth of prestressing tendon;  $e_m$  = eccentricity of tendon at midspan;  $e_s$  = eccentricity of prestressing tendon at support;  $f'_c$  = concrete compressive strength;  $f_{pe}$  = effective stress of the prestressing tendon;  $f_{pu}$  = ultimate stress of prestressing tendon;  $L$  = length of beam;  $\rho_s$  = tensile-steel reinforcement ratio. 1 mm = 0.0394 in.; 1 MPa = 0.145 ksi.

From Table 12 and Fig. 5 and 6, the following observations were made.

- The ratio of  $\Delta P_{us} / \Delta P_{u, pred}$  has a smaller average value, standard deviation, and coefficient of variation when

the ratio of compression-stress-block depths  $K$  is based on Eq. (11).

- The predicted increase in load-carrying capacity based on refined equations is in good agreement with

**Table 8.** Characteristics of simple-span beams studied by Du and Tao

Beam marking	$\rho_{st}$ %	$f'_c$ , MPa	$A_{pst}$ mm <sup>2</sup>	$f_{pe}$ MPa	$f_{pu}$ MPa	$e_s$ mm	$e_m$ mm	$L/d_p$	Profile*	Load type†
A-1	0.39	30.6	58.8	960	1790	80	80	19.1	S	T
A-2	0.39	30.6	98.0	904	1790	80	80	19.1	S	T
A-3	0.59	30.6	156.8	820	1790	80	80	19.1	S	T
A-4	0.39	30.6	58.8	869	1790	80	80	19.1	S	T
A-5	0.77	30.6	78.4	810	1790	80	80	19.1	S	T
A-6	1.16	30.6	156.8	854	1790	80	80	19.1	S	T
A-7	0.77	30.6	39.2	885	1790	80	80	19.1	S	T
A-8	1.16	33.1	58.8	894	1790	80	80	19.1	S	T
A-9	2.01	33.1	156.8	920	1790	80	80	19.1	S	T
B-1	0.39	45.8	58.8	1008	1840	80	80	19.1	S	T
B-2	0.39	45.8	98.0	987	1840	80	80	19.1	S	T
B-3	0.59	42.5	156.8	963	1840	80	80	19.1	S	T
B-4	0.39	42.5	58.8	1040	1840	80	80	19.1	S	T
B-5	0.77	42.5	78.4	989	1840	80	80	19.1	S	T
B-6	1.16	42.5	137.2	1002	1840	80	80	19.1	S	T
B-7	0.77	48.8	39.2	1002	1840	80	80	19.1	S	T
B-8	1.16	42.5	58.8	1002	1840	80	80	19.1	S	T
B-9	2.01	48.8	98.0	1050	1840	80	80	19.1	S	T
C-1	0.39	33.1	58.8	905	1790	80	80	19.1	S	T
C-3	0.59	33.1	156.8	825	1790	80	80	19.1	S	T
C-7	0.77	33.1	39.2	955	1790	80	80	19.1	S	T
C-9	2.01	33.1	156.8	903	1790	80	80	19.1	S	T

Source: Data from Du and Tao 1985.

\*S = straight.

†T = two-point loads.

Note:  $A_{ps}$  = area of prestressing tendon;  $d_p$  = effective depth of prestressing tendon;  $e_m$  = eccentricity of tendon at midspan;  $e_s$  = eccentricity of prestressing tendon at support;  $f'_c$  = concrete compressive strength;  $f_{pe}$  = effective stress of the prestressing tendon;  $f_{pu}$  = ultimate stress of prestressing tendon;  $L$  = length of beam;  $\rho_s$  = tensile-steel reinforcement ratio. 1 mm = 0.0394 in.; 1 MPa = 0.145 ksi.

the observed values (Fig. 5 and 6). Alternatively, the predictions using simplified equations are conservative (Fig. 5 and 6).

- Table 12 shows that omitting beams with  $cl/d_s > 0.375$ ,  $L/d_p > 20$ ,  $f_{pe} < 0.4f_{pu}$  and without deviators leads to a higher mean of  $\Delta P_{us}/\Delta P_{u,pred}$ .

- Naaman Eq. (28) for  $f_{ps}$  gives a mean  $\Delta P_{us}/\Delta P_{u,pred}$  close to 1, whereas the use of ACI 318-08 Eq. (22) for  $f_{ps}$  leads to the smallest coefficient of variation for  $\Delta P_{us}/\Delta P_{u,pred}$ .



**Table 9.** Characteristics of simple-span beams studied by Tam and Pannell

Beam marking	$\rho_s$ , %	$f'_c$ , MPa	$A_{ps}$ , mm <sup>2</sup>	$f_{pe}$ , MPa	$f_{pu}$ , MPa	$e_s$ , mm	$e_m$ , mm	$L/d_p$	Profile*	Load type†
B1	0.48	51.8	154.8	778	1622	55	55	18.0	S	S
B2	0.98	48.6	232.2	747	1622	68	68	23.5	S	S
B3	0.56	57.6	116.1	847	1622	43	43	27.5	S	S
B4	0.85	42.3	193.5	864	1622	39.5	39.5	28.6	S	S
B5	0.74	53.1	116.1	947	1622	25	25	29.3	S	S
B6	0.71	56.7	154.8	853	1622	18	18	31.4	S	S
B7	0.71	48.4	154.8	778	1622	24	24	38.8	S	S
B8	1.05	52.1	77.4	656	1622	14	14	43.0	S	S

Source: Data from Tam and Pannell 1976.

\*S = straight.

†S = single-point load.

Note:  $A_{ps}$  = area of prestressing tendon;  $d_p$  = effective depth of prestressing tendon;  $e_m$  = eccentricity of tendon at midspan;  $e_s$  = eccentricity of prestressing tendon at support;  $f'_c$  = concrete compressive strength;  $f_{pe}$  = effective stress of the prestressing tendon;  $f_{pu}$  = ultimate stress of prestressing tendon;  $L$  = length of beam;  $\rho_s$  = tensile-steel reinforcement ratio. 1 mm = 0.0394 in.; 1 MPa = 0.145 ksi.

**Table 10.** Characteristics of simple-span beams studied by Campbell and Chouinard

Beam marking	$\rho_s$ , %	$f'_c$ , MPa	$A_{ps}$ , mm <sup>2</sup>	$f_{pe}$ , MPa	$f_{pu}$ , MPa	$e_s$ , mm	$e_m$ , mm	$L/d_p$	Profile*	Load type†
2	0.49	32.4	148.4	1065	1760	80	80	15.0	S	T
3	0.98	31.6	148.4	1049	1760	80	80	15.0	S	T
4	1.46	37.1	148.4	1096	1760	80	80	15.0	S	T
5	1.95	37.4	148.4	1081	1760	80	80	15.0	S	T
6	2.44	37.4	148.4	1086	1760	80	80	15.0	S	T

Source: Data from Campbell and Chouinard 1991.

\*S = straight.

†T = two-point loads.

Note:  $A_{ps}$  = area of prestressing tendon;  $d_p$  = effective depth of prestressing tendon;  $e_m$  = eccentricity of tendon at midspan;  $e_s$  = eccentricity of prestressing tendon at support;  $f'_c$  = concrete compressive strength;  $f_{pe}$  = effective stress of the prestressing tendon;  $f_{pu}$  = ultimate stress of prestressing tendon;  $L$  = length of beam;  $\rho_s$  = tensile-steel reinforcement ratio. 1 mm = 0.0394 in.; 1 MPa = 0.145 ksi.

## Recommendation on the use of proposed equations

This paper proposes refined equations (Eq. [13]–[15]) and simplified equations (Eq. [19]–[21]) to relate the tendon force  $F_{ps}$  and tendon eccentricity at midspan  $e_m$  with an increase in load-carrying capacity for simple-span beams.

The refined equations require the value of the ratio of compression-stress-block depths  $K$ , which can be obtained from Eq. (9) or (11). Also, the tendon force  $F_{ps}$  depends on the tendon area  $A_{ps}$  and tendon stress  $f_{ps}$ , the latter of which can be evaluated by Eq. (22), (24), or (28).

**Table 11.** Characteristics of simple-span beams studied by Kobayashi and Nieda

Beam marking	$\rho_s$ , %	$f'_c$ , MPa	$A_{ps}$ , mm <sup>2</sup>	$f_{pe}$ , MPa	$f_{pu}$ , MPa	$e_s$ , mm	$e_m$ , mm	$L/d_p$	Profile*	Load type†
No. 2	0.22	40.8	132.7	846	1080	40	40	12.1	S	T
No. 4	1.04	38.3	132.7	724	1080	40	40	12.1	S	T
No. 6	0.22	40.8	227.0	721	1180	40	40	12.1	S	T
No. 8	0.22	38.2	227.0	721	1180	40	40	12.1	S	T
No. 11	0.22	64.1	227.0	719	1180	40	40	12.1	S	T
No. 13	1.58	62.7	227.0	664	1180	40	40	12.1	S	T
No. 15	0.22	64.1	415.5	721	1180	40	40	12.1	S	T
No. 17	0.22	64.1	415.5	828	1180	40	40	12.1	S	T

Source: Data from Kobayashi and Nieda 1991.

\*S = straight.

†T = two-point loads.

Note:  $A_{ps}$  = area of prestressing tendon;  $d_p$  = effective depth of prestressing tendon;  $e_m$  = eccentricity of tendon at midspan;  $e_s$  = eccentricity of prestressing tendon at support;  $f'_c$  = concrete compressive strength;  $f_{pe}$  = effective stress of the prestressing tendon;  $f_{pu}$  = ultimate stress of prestressing tendon;  $L$  = length of beam;  $\rho_s$  = tensile-steel reinforcement ratio. 1 mm = 0.0394 in.; 1 MPa = 0.145 ksi.

Depending on the purpose and the availability of section and material properties of the beam, the proposed equations can be used appropriately as follows:

- Case A: If the material properties of the beam are unknown or are in preliminary strengthening design, the simplified equations together with ACI 318-08's equation (Eq. [22]) for  $f_{ps}$  can be used to determine the tendon area required for a specified increase in load-carrying capacity of a beam.
- Case B: If the section and material properties of the beam are known, the refined equations with the upper-limit value of  $K = 0.375\beta_1d_s/a_0$  [Eq. (9)] can be used to determine the required tendon area for a specified increase in load-carrying capacity of a beam.
- Case C: If the tendon area has been provided and the section and material properties of the beam are available, the refined equations with the upper limit value of  $K = 1 + \chi(d_p/d_s)$  [Eq. (11)] can be used to evaluate the increase in load-carrying capacity of a beam.

The refined equations give a safety margin equivalent to a load factor of about 1.3 to 1.4 with a coefficient of variation of 0.3, whereas the simplified equations give a safety margin equivalent to a load factor of about 3 (Table 12) and a coefficient of variation of 0.4. The following section gives an example illustrating the use of the proposed equations for the discussed cases.

### Example problem

The simple-span, 8-m-long (26.25 ft) T-beam in **Fig. 7** is subjected to uniform loading and is to be strengthened to carry 30% more load than its original load-carrying capacity. The following information is given:

$$A_s = 2250 \text{ mm}^2 (3.49 \text{ in.}^2)$$

$$b = 500 \text{ mm (19.69 in)}$$

$$d_s = 450 \text{ mm (17.72 in)}$$

$$f'_c = 30 \text{ MPa (4.35 ksi)}$$

$$f_y = 460 \text{ MPa (66.72 ksi)}$$

$$L = 8000 \text{ mm (26.25 ft)}$$

Before strengthening, the depth of concrete compression block at ultimate flexural strength limit state is determined by Eq. (2).

$$a_0 = \frac{A_s f_y}{0.85 f'_c b} = \frac{(2250)(460)}{(0.85)(30)(500)} = 81.2 \text{ mm (3.20 in.)}$$

This is less than the flange thickness of 150 mm (6 in.) and, hence, rectangular section behavior.

From section 10.2.73 of ACI 318-08,

$$\beta_1 = 0.85 - 0.05 \left( \frac{30 - 28}{7} \right) = 0.84$$

The nominal moment capacity of the beam  $M_n$  is determined by Eq. (34).

$$\begin{aligned} M_n &= A_s f_y \left( d_s - \frac{a_0}{2} \right) \\ &= (2250)(460) \left( 450 - \frac{81.2}{2} \right) (10^{-6}) \\ &= 423.7 \text{ kN-m (312.5 kip-ft)} \end{aligned} \quad (34)$$

The nominal load-carrying capacity of the beam under uniform load would be 423.7 kN (95.3 kip). Thus, the required increase in load-carrying capacity is 30% of that or 127.1 kN (28.6 kip).

Assuming that the beam is to be strengthened using external tendons, the following properties are given:

$$E_{ps} = 195,000 \text{ MPa (28,281 ksi)}$$

$$f_{pu} = 1900 \text{ MPa (275.5 ksi)}$$

$$f_{py} = 1786 \text{ MPa (259 ksi)}$$

To ensure satisfactory performance of strengthened beams in serviceability and ultimate limit states, the effective tendon depth  $d_p$  should be from 0.65 to 0.90 times the overall beam height. The effective tendon prestress  $f_{pe}$  should be from 0.40 to 0.65 times the tendon strength.<sup>11</sup> Therefore, adopt the following:

$$d_p = 425 \text{ mm (16.73 in)}, \text{ giving } e_m = 247.1 \text{ mm (9.73 in)}$$

$$f_{pe} = 950 \text{ MPa (137.78 ksi)}$$

As the beam is carrying uniform load, parabolic tendons will be provided.

### Case A: Preliminary or simplified design

In this case, the material parameters of the original beam are unknown, and the desired increase in load-carrying capacity could have been determined from the desired increase in design loads. Because  $L/d_p = 18.8 < 35$ , the tendon stress based on the ACI 318-08 equation (Eq. [22]) is calculated.

$$f_{ps} = f_{pe} + 68.95 + \frac{f'_c}{B\rho_p} \quad \text{where } \rho_p = \frac{A_{ps}}{bd_p}$$

**Table 12.** Comparison of predicted load increase with test results

Sample size (number of beams)		$K = \frac{0.375\beta_1 d_s}{a_0}$ (Eq. [9])					
		Refined Eq. (13), (14), and (15)			Simplified Eq. (19), (20), and (21)		
		$\frac{\Delta P_{us}}{\Delta P_{u11}}$	$\frac{\Delta P_{us}}{\Delta P_{u12}}$	$\frac{\Delta P_{us}}{\Delta P_{u13}}$	$\frac{\Delta P_{us}}{\Delta P_{u21}}$	$\frac{\Delta P_{us}}{\Delta P_{u22}}$	$\frac{\Delta P_{us}}{\Delta P_{u23}}$
All beams (124)	Mean	1.40	1.43	1.40	3.07	3.13	3.09
	Standard deviation	0.40	0.48	0.47	1.21	1.35	1.40
	COV	0.29	0.34	0.34	0.39	0.43	0.45
Beams* (98)	Mean	1.48	1.52	1.49	3.29	3.40	3.36
	Standard deviation	0.37	0.46	0.44	1.17	1.32	1.38
	COV	0.25	0.30	0.30	0.36	0.39	0.41

\* All beams except for beams with  $c/d_s > 0.375$ , with  $L/d_p > 20$  and without deviator, or with  $f_{pe} < 0.4f_{pu}$

Note:  $a_0$  = depth of equivalent rectangular stress block for unstrengthened beam;  $c$  = neutral-axis depth of strengthened beam at critical midspan section;  $COV$  = coefficient of variation;  $d_p$  = effective depth of prestressing tendon;  $d_s$  = effective depth of mild-steel reinforcement;  $f_{pe}$  = effective stress of the prestressing tendon;  $f_{pu}$  = ultimate stress of prestressing tendon;  $K$  = ratio of compression-stress-block depths;  $L$  = length of beam;  $X = 1, 2, \text{ or } 3$ , indicating the equations with which the tendon stress is evaluated—that is, ACI 318-08 Eq. (22), MacGregor Eq. (24), or Naaman Eq. (28)], respectively;  $\beta_1$  = factor to determine the depth of equivalent rectangular stress block;  $\Delta P_{us}$  = observed increase in load-carrying capacity;  $\Delta P_{u1X}$  = predicted increase in load-carrying capacity based on refined equations;  $\Delta P_{u2X}$  = predicted increase in load-carrying capacity based on simplified equations;  $\beta_1$  = factor to determine the depth of equivalent rectangular stress block;  $\chi$  = relative prestressing index.

$$= 950 + 68.95 + \frac{30}{100 \left( \frac{A_{ps}}{500(425)} \right)}$$

Substituting the value of  $A_{ps}f_{ps}$  for  $F_{ps}$  into simplified Eq. (21) gives

$$\Delta P_u = 127,100 N = \frac{8F_{ps}e_m}{L} = 8A_{ps}f_{ps} \frac{e_m}{L}$$

$$= 8A_{ps} \left( 950 + 68.95 + \frac{30}{100 \left( \frac{A_{ps}}{500(425)} \right)} \right) \left( \frac{247.1}{8000} \right)$$

$$\Rightarrow A_{ps} = 442.2 \text{ mm}^2 (0.69 \text{ in.}^2)$$

### Case B: Refined design

In this case, the section and material parameters of the original beam are available. Using Eq. (9),

$$K = \frac{0.375\beta_1 d_s}{a_0} = \frac{(0.375)(0.84)(450)}{81.2} = 1.75$$

The tendon stress can be based on Eq. (22), (24), or (28).

Using Eq. (24),

$$f_{ps} = f_{pe} + 0.0315E_{ps} \frac{d_p - Ka_0 / \beta_1}{L}$$

$$= 950 + (0.0315)(195,000) \left[ \frac{425 - 1.75(81.2 / 0.84)}{8000} \right]$$

$$= 1146 \text{ N/mm}^2 (166.3 \text{ ksi})$$

Substituting into refined Eq. (15) gives

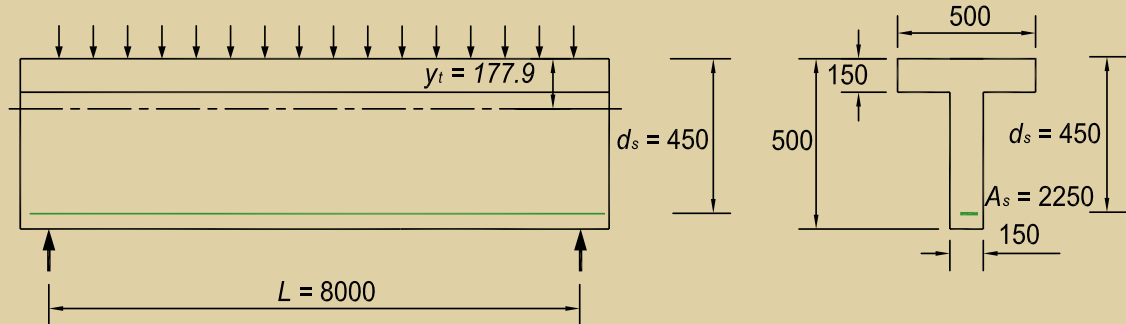
$$\Delta P_u = 127,100 = \frac{8F_{ps}e_m}{L} + \frac{8F_{ps} \left[ y_t - \frac{a_0}{2}(1+K) \right]}{L}$$

$$= (8)(A_{ps})(1146) \left\{ \frac{247.1}{8000} + \left[ \frac{177.9 - \frac{81.2}{2}(1+1.75)}{8000} \right] \right\}$$

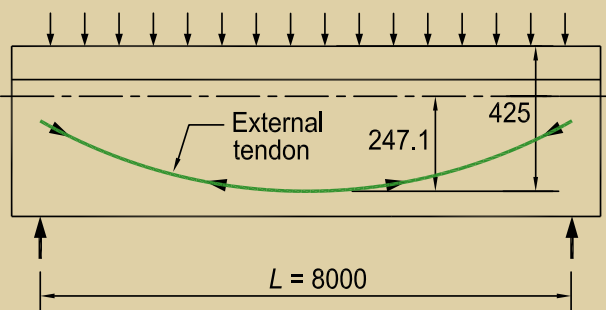
$$\Rightarrow A_{ps} = 353.8 \text{ mm}^2 (0.55 \text{ in.}^2)$$

Compared with the results from case A, a smaller tendon area is needed because the simplified equation is more conservative, as previously noted.

Sample size (number of beams)		$K = 1 + \chi \frac{d_p}{d_s}$ (Eq. [11])					
		Refined Eq. (13), (14), and (15)			Simplified Eq. (19), (20), and (21)		
		$\frac{\Delta P_{us}}{\Delta P_{u11}}$	$\frac{\Delta P_{us}}{\Delta P_{u12}}$	$\frac{\Delta P_{us}}{\Delta P_{u13}}$	$\frac{\Delta P_{us}}{\Delta P_{u21}}$	$\frac{\Delta P_{us}}{\Delta P_{u22}}$	$\frac{\Delta P_{us}}{\Delta P_{u23}}$
All beams (124)	Mean	1.34	1.31	1.22	3.07	3.03	2.82
	Standard deviation	0.35	0.39	0.36	1.21	1.28	1.26
	COV	0.27	0.29	0.29	0.39	0.42	0.45
Beams* (98)	Mean	1.38	1.36	1.25	3.29	3.26	3.02
	Standard deviation	0.33	0.38	0.34	1.17	1.27	1.27
	COV	0.24	0.28	0.27	0.36	0.39	0.42



Before strengthening



Layout of external tendon

**Figure 7.** This drawing shows the simple-span T-beam under uniform load used for the example. Note: All dimensions are in millimeters.  $A_s$  = area of tensile-steel reinforcement;  $d_s$  = effective depth of tensile-steel reinforcement;  $L$  = length of beam;  $y_t$  = distance between extreme compressive fiber and centroidal axis of beam before cracking. 1 mm = 0.0394 in.

### Case C: Evaluation of increase in load-carrying capacity

In this case, the tendon properties are known in addition to those of the original beam. Again, the tendon stress can be evaluated using Eq. (22), (24), or (28). As an illustration, Eq. (28) is used. Because the value  $\epsilon_{ce}$  is small compared with the other terms, it will be omitted. From Eq. (27),

$$\Omega_u = \frac{5.4}{L/d_p} = \frac{5.4}{8000/425} = 0.287$$

From Eq. (28),

$$\begin{aligned} f_{ps} &= f_{pe} + \Omega_u E_{ps} \epsilon_{ce} + \Omega_u E_{ps} \left( \frac{d_p \beta_1}{K a_0} - 1 \right) \epsilon_{cu} \\ &= 950 + (0.287)(195,000) \left[ \frac{(425)(0.84)}{(1.75)(81.2)} - 1 \right] (0.003) \\ &= 1204 \text{ N/mm}^2 \text{ (174.6 ksi)} \end{aligned}$$

Based on the following values,  $\rho_p$ ,  $\rho_s$ , and  $\chi$  can be calculated.

$$A_{ps} = 353.8 \text{ mm}^2 \text{ (0.55 in.}^2\text{)}$$

$$A_s = 2250 \text{ mm}^2 \text{ (3.49 in.}^2\text{)}$$

$$d_p = 425 \text{ mm (16.73 in.)}$$

$$d_s = 450 \text{ mm (17.22 in.)}$$

$$\rho_p = \frac{A_{ps}}{b d_p} = \frac{353.8}{(500)(425)} = 0.17\%$$

$$\rho_s = \frac{A_s}{b d_s} = \frac{2250}{(500)(450)} = 1\%$$

$$\chi = \frac{\rho_p f_{py}}{\rho_s f_y} = \frac{(0.17)(1786)}{(1)(460)} = 0.66$$

Thus, from Eq. (11),

$$K = 1 + (0.66) \left( \frac{425}{450} \right) = 1.62$$

Substituting  $f_{ps}$ ,  $K$ , and  $A_{ps} = 353.8 \text{ mm}^2$  (0.55 in.<sup>2</sup>) into refined Eq. (15) gives

$$\begin{aligned} \Delta P_u &= \frac{8F_{ps}e_m}{L} + \frac{8F_{ps} \left[ y_t - \frac{a_0}{2}(1+K) \right]}{L} \\ &= (8)(353.8)(1204) \\ &\quad \times \left\{ \frac{247.1}{8000} + \frac{\left[ 177.9 - \left( \frac{81.2}{2} \right)(1+1.62) \right]}{8000} \right\} (10^{-3}) \\ &= 135.7 \text{ kN (30.5 kip)} > 127.1 \text{ kN (28.6 kip)} \end{aligned}$$

Alternatively, by substituting  $f_{ps}$  and  $A_{ps} = 442.2 \text{ mm}^2$  (0.69 in.<sup>2</sup>) into Eq. (21), the increase in load-carrying capacity based on the simplified equation would be

$$\begin{aligned} \Delta P_u &= \frac{8F_{ps}e_m}{L} = \frac{(8)(442.2)(1204)(247.1)}{8000} (10^{-3}) \\ &= 131.6 \text{ kN (29.6 kip)} > 127.1 \text{ kN (28.6 kip)} \end{aligned}$$

## Conclusion

In this study, equations were established for the direct determination of external tendon area and eccentricity to strengthen a simple-span, reinforced concrete beam. The refined equations were derived uniquely from moment equilibrium at the critical midspan section as well as from strut-and-tie models.

The increase in load-carrying capacity has two components:

- the component balanced directly by the tendons
- the component due to the increased concrete compression zone

By neglecting the latter component, a set of simplified equations, which is independent of the material properties of the beam to be strengthened, was obtained.

Compared with the test results of 124 simple-span beams reported in the literature, the refined equations underestimated the increase in load-carrying capacity up to 40%, whereas the simplified equations underestimated the same by as much as 65%.

The simplified equations with ACI 318-08 equations for tendon stress can be used in preliminary design to determine the tendon area, while the refined equations can be used to directly evaluate the increase in load-carrying capacity due to the provision of external tendons.

## References

1. Aalami, B. O., and D. T. Swanson. 1988. Innovative Rehabilitation of a Parking Structure. *Concrete International*, V. 10, No. 2 (February): pp. 30–35.
2. Alkhairi, F. M. 1991. On the Flexural Behavior of Concrete Beams Prestressed with Unbonded Internal and External Tendons. PhD thesis, University of Michigan, Ann Arbor.
3. Naaman, A. E., and F. M. Alkhairi. 1991. Stress at Ultimate in Unbonded Post-Tensioning Tendons: Part 2—Proposed Methodology. *ACI Structural Journal*, V. 88, No. 6 (November–December): pp. 683–692.
4. Naaman, A. E., N. Burns, C. French, W. Gamble, and A. H. Mattock. 2002. Stress in Unbonded Prestressing Tendons at Ultimate: Recommendation. *ACI Structural Journal*, V. 99, No. 4 (July–August): pp. 520–531.
5. American Concrete Institute (ACI) Committee 318. 2008. *Building Code Requirements for Structural Concrete (ACI 318-08) and Commentary (ACI 318R-08)*. Farmington Hills, MI: ACI.
6. American Association of State and Highway Transportation Officials (AASHTO). 2004. *AASHTO LRFD Bridge Design Specifications*. 3rd ed. Washington DC: AASHTO.
7. Lin, T. Y. 1963. Load-Balancing Method for Design and Analysis of Prestressed Concrete Structures. *Journal of the American Concrete Institute*, V. 60, No. 6 (June): pp. 719–741.
8. Roberts-Wollmann, C. L., M. E. Kreger, D. M. Rogovsky, and J. E. Breen. 2005. Stress in External Tendons at Ultimate. *ACI Structural Journal*, V. 102, No. 2 (March–April): pp. 206–213.
9. Roberts-Wollmann, C. L., M. E. Kreger, D. M. Rogovsky, J. E. Breen, J. S. Du, W. L. Lu, and W. Y. Ji. Discussion. 2006. *ACI Structural Journal*, V. 103, No. 1 (January–February): pp. 149–154.

10. Tan K. H., and C. K. Ng. 1997. Effects of Deviators and Tendon Configuration on Behavior of Externally Prestressed Beams. *ACI Structural Journal*, V. 94, No. 1 (January–February): pp. 13–22.
11. Tan, K. H., A. E. Naaman, M. A. Mansur, and C. K. Ng. 1997. External Prestressing in Structures. Final report RP 930647, Department of Civil Engineering, National University of Singapore.
12. Tan, K. H. 2006. Strengthening of RC Beams Based on Load-Balancing Method. CD-ROM. In *Proceedings of The International Conference on Civil Engineering Infrastructure Systems (CEIS 2006), June 12–14, 2006, American University of Beirut, Beirut-Lebanon*. Beirut, Lebanon: Arabic Scientific Publisher, Beirut.
13. Harajli, M. H. 1993. Strengthening of Concrete Beams by External Prestressing. *PCI Journal*, V. 38, No. 6 (November–December): pp. 76–88.
14. Khairallah, N., and M. H. Harajli. 1997. Experimental Evaluation of the Behavior of Reinforced Concrete Beams Strengthened Using External Prestressing. CD-ROM. In *Proceedings of The International Conference on Rehabilitation and Development of Civil Engineering Infrastructure Systems, June 9–11, 1997, American University of Beirut, Beirut-Lebanon*, pp. 1282–1293. Beirut, Lebanon: Arabic Scientific Publisher, Beirut.
15. Harajli, M. H., and M. Y. Kanj. 1991. Ultimate Flexural Strength of Concrete Members Prestressed With Unbonded Tendons. *ACI Structural Journal*, V. 88, No. 6 (November–December): pp. 663–673.
16. Harajli, M. H., and M. Y. Kanj. 1992. Service Load Behavior of Concrete Members Prestressed With Unbonded Tendons. *Journal of Structural Engineering*, V. 118, No. 9 (September): pp. 2569–2589.
17. Chakrabarti, P. R., and T. P. Whang. 1989. Study of Partially Prestressed Beams with Unbonded Post-Tensioning. In *Structural Design, Analysis and Testing, Proceedings of the Sections Related to Design, Analysis and Testing at Structures Congress '89, May 1-5, 1989*, pp. 189–200. New York, NY: American Society of Civil Engineers.
18. Chakrabarti, P. R., T. P. Whang, W. Brown, K. M. Arsad, and E. Amezeua. 1994. Unbonded Post-tensioning Tendons and Partially Prestressed Beams. *ACI Structural Journal*, V. 91, No. 5 (September–October): pp. 616–625.
19. Chakrabarti, P. R. 1995. Ultimate Stress for Unbonded Post-Tensioning Tendons in Partially Prestressed Beams. *ACI Structural Journal*, V. 92, No. 6 (November–December): pp. 689–697.
20. Du, G. C., and X. K. Tao. 1985. Ultimate Stress of Unbonded Tendons in Partially Prestressed Concrete Beams. *PCI Journal*, V. 30, No. 6 (November–December): pp. 72–91.
21. Tam, A., and F. N. Pannell. 1976. The Ultimate Moment Resistance of Unbonded Partially Prestressed Reinforced Concrete Beams. *Magazine of Concrete Research*, V. 28, No. 97 (December): pp. 203–208.
22. Campbell, T. I., and K. L. Chouinard. 1991. Influence of Nonprestressed Reinforcement on The Strength of Unbonded Partially Prestressed Concrete Members. *ACI Structural Journal*, V. 88, No. 5 (September–October): pp. 546–551.
23. Kobayashi, K., and T. Nieda. 1991. Flexural Behavior of Unbonded Post-Tensioned Prestressed Concrete Beams. In *Modern Application of Prestressed Concrete: Proceedings of the International Symposium on Modern Applications of Prestressed Concrete, V. 2*, pp. 250–257. Beijing, China: International Academic Publisher.

## Notation

$a$	= depth of equivalent rectangular stress block for strengthened beam
$a_0$	= depth of equivalent rectangular stress block for unstrengthened beam
$A_{ps}$	= area of prestressing steel
$A_s$	= area of tensile-steel reinforcement
$b$	= beam width
$B$	= constant
$c$	= neutral-axis depth of strengthened beam at critical midspan section
$C$	= constant
$d_p$	= effective depth of prestressing tendon
$d_s$	= effective depth of tensile-steel reinforcement
$e_m$	= eccentricity of prestressing tendon at midspan
$e_s$	= eccentricity of prestressing tendon at support



$E_{ps}$	= elastic modulus of prestressing tendon	$\Delta P_{u, pred}$	= predicted increase in load-carrying capacity of strengthened beam
$f'_c$	= concrete compressive strength	$\Delta P_{us}$	= observed increase in load-carrying capacity
$f_{pe}$	= effective stress of the prestressing tendon	$\Delta P_{u1X}$	= predicted increase in load-carrying capacity based on refined equations, where $X$ is equal to 1, 2, or 3, indicating equations with which tendon stress is evaluated—that is, ACI 318-08 Eq. (22), MacGregor Eq. (24), or Naaman Eq. (28), respectively
$f_{ps}$	= prestressing tendon stress at ultimate limit state	$\Delta P_{u2X}$	= predicted increase in load-carrying capacity based on simplified equations, where $X$ is equal to 1, 2, or 3, indicating equations with which tendon stress is evaluated—that is, ACI 318-08 Eq. (22), MacGregor Eq. (24), or Naaman Eq. (28), respectively
$f_{pu}$	= ultimate stress of prestressing tendon	$\Delta w_u$	= increase in uniform load
$f_{py}$	= yield stress of prestressing tendon	$\epsilon_{ce}$	= precompression strain in the concrete at tendon level
$f_y$	= yield strength of tensile-steel reinforcement	$\epsilon_{cu}$	= ultimate concrete compression strain
$F_c$	= concrete strut force	$\theta$	= angle between tendon and centroidal axis of the beam
$F_{ps}$	= prestressing tendon force at ultimate limit state	$\rho_p$	= prestressing reinforcement ratio
$K$	= ratio of compression-stress-block depths	$\rho_s$	= tensile-steel reinforcement ratio
$l$	= distance from point load to nearest support	$\chi$	= relative prestressing index
$L$	= length of beam	$\Omega_u$	= bond reduction factor
$M_n$	= nominal moment capacity		
$M_{n0}$	= moment capacity of unstrengthened beam		
$M_{ns}$	= moment capacity of strengthened beam		
$n$	= distance from draped point to nearest support		
$P_{u0}$	= load-carrying capacity of unstrengthened beam		
$P_{us}$	= load-carrying capacity of strengthened beam from testing		
$T_0$	= tensile force of reinforcement		
$w_{u0}$	= uniform load-carrying capacity of unstrengthened beam		
$y_t$	= distance between extreme compressive fiber and centroidal axis of beam before cracking		
$\beta_1$	= factor to determine depth of equivalent rectangular stress block		
$\gamma$	= angle between strut and centroidal axis of the beam		
$\gamma_1$	= angle between straight tendon and inclined strut for strengthened beam		
$\Delta M_n$	= increase in moment capacity of strengthened beam		
$\Delta P_u$	= increase in load-carrying capacity due to addition of external tendons		



## About the authors



Kiang Hwee Tan, DrEng, P.Eng., is an associate professor for the Department of Civil Engineering at the National University of Singapore in Singapore.



DeCheng Kong is a PhD candidate for the Department of Civil Engineering at National University of Singapore.

## Synopsis

External post-tensioning, in which external tendons are installed on the outside of a beam, is an efficient strengthening method for concrete beams. In such cases, a direct approach to determine the tendon configuration for a desired increase in load-carrying capacity would be useful, and this paper develops just such an approach for simple-span beams. The installation of external tendons causes an increase in the beam capacity in two ways. First, the tendons contribute directly to the load-carrying capacity by balancing part of the increased loads. Second, the concrete compression zone is increased, which indirectly leads to an increase in the beam capacity.

Two sets of equations—refined equations and simplified equations—are established for the determination of the increase in load-carrying capacity. The refined equations account for the contribution of both the increased concrete compression zone and the direct contribution of the tendons, while the simplified equations account for the direct contribution of the tendons only. A comparison with 124 simple-span beams from previous investigations showed that the increases in load-carrying capacity predicted by the refined equations are in good agreement with the test data, while those predicted by the simplified equations are conservative.

## Keywords

Beam, external post-tensioning, load balancing, load-carrying capacity, structural strengthening.

## Review policy

This paper was reviewed in accordance with the Precast/Prestressed Concrete Institute's peer-review process.

## Reader comments

Please address any reader comments to *PCI Journal* editor-in-chief Emily Lorenz at [elorenz@pci.org](mailto:elorenz@pci.org) or Precast/Prestressed Concrete Institute, c/o *PCI Journal*, 209 W. Jackson Blvd., Suite 500, Chicago, IL 60606. 